Extracellular potentials generated by axonal projections are shaped by patterns of bifurcations and terminations

Thomas McColgan, Hermann Wagner, Richard Kempter

September 15, 2015

Introduction

Extracellular field potentials (EFPs) in the brain were long thought to be primarily synaptic in origin (Buzsáki et al., 2012). The study of the fields is relevant for the interpretation of data collected with measurement methods which rely on the extracellular field potential (Brette and Destexhe, 2012). Extracellular fields are also at the base of many noninvasive measurement methods (Nunez and Srinivasan, 2006), where the underlying mechanisms of far field generation are often poorly understood (Rattay and Danner, 2014).

Many modelling studies focus on the extracellular fields induced by currents on the dendrites and soma of the postsynaptic neuron (Holt and Koch, 1999; Gold et al., 2006; Lindén et al., 2010, 2011; Einevoll et al., 2013). However, a number of recent data analysis and modeling studies have revealed that active, non-synaptic membrane currents can play a role in generating EFPs (Reimann et al., 2013).

The aim of this study is to understand how the EFP is influenced by the anatomical structure of the axons. In particular, we explain how typical projection patterns in which an axon bundle widens and then terminates in its projection area affect the EFP. Such axon bundles, sometimes called nerves or facicles, exist throughout the peripheral and central nervous system (Nornes and Das, 1972; Goodman et al., 1984; Hentschel and Ooyen, 1999; Kandel et al., 2000). The white matter of the brain can be viewed as an agglomeration of such bundles (Schüz and Braitenberg, 2002).

It has been shown (Kuokkanen et al., 2010; Denker et al., 2011; Lindén et al., 2011) that with sufficient spatial and temporal organization extracellular fields of axonal and synaptic sources can reach strengths on the order of several mV. Here we extend this finding to include more general axon bundles, including those receiving input with less temporal precision.

We characterize three principal effects of axon bundle structure on the EFP. These effects are elaborations of the properties described in past (Plonsey, 1977; Gydikov and Trayanova, 1986; Gydikov et al., 1986) for peripheral nerves. We find that the low-frequency components of the EFP are governed by the local density of bifurcations and terminations. The high-frequency components are governed by the local fiber density. Furthermore we show that the low-frequency components exceed the high-frequency components in spatial reach.

We demonstrate these properties using two models of varying complexity, both of them based on a forward model of the extracellular field potential (Holt and Koch, 1999; Gold et al., 2006). The

first model includes a detailed multicompartment model of the axon population. The second is an analytically tractable simplification of the axon bundle. Finally, we demonstrate the properties in real data using as a set of in-vivo electrophysiological recordings from the barn owl brain stem.

- cite: rall, Rinzel, Goldwyn, Einevoll, Destexe, Brette book, nunez&srinivasan, telenzuk
- Some more refs to add:Schomburg et al 2011 Ray Maunsell 2011, Belluscio 2012, Weiss 2010)

Results

- Axonal projections generate a dipole-like field potential (**Fig 1A**)
  - long range
  - low frequency
  - Examples of phenomenology from literature
- General results for axonal projections :
  - The low-frequency (eg population rate pulse) parts are governed by the local density of bifurcations and terminations(**Fig 1B**)
  - The high-frequency (eg individual spikes, 'noise', neurophonic) parts are governed by the local fiber density(**Fig 1C**)
  - The low-frequency component exceeds the high-frequency component in reach (**Fig 2**)
- The barn owl neurophonic as an example that shows these properties(**Fig 3**)
  - The high-frequency component shows a steady increase in latency along the projections' depth, while the low-frequency can have stationary parts caused by sharp increases or decreases of fiber number (bifurcations or terminations).
  - These aspects are reflected in the model
- Ways of understanding the effect
  - Single AP along single axon(**Fig 4**)
  - Analytical model(**Fig 5**)

Discussion

- Relevance of Findings
  - Interpretation of CSD
    - Classical CSD: constant fiber density, variable currents
    - Here: variable fiber density, constant currents
  - Dipole has far field, ABR response?
- Compare to other auditory systems (Chicken NL, MSO)
  - Speculate on functional relevance of polarity shift (a la Rinzel & Goldwyn)
- compare to other fiber bundle systems

Methods

- Experimental Methods
- Multicompartment Model
- Analytical Model

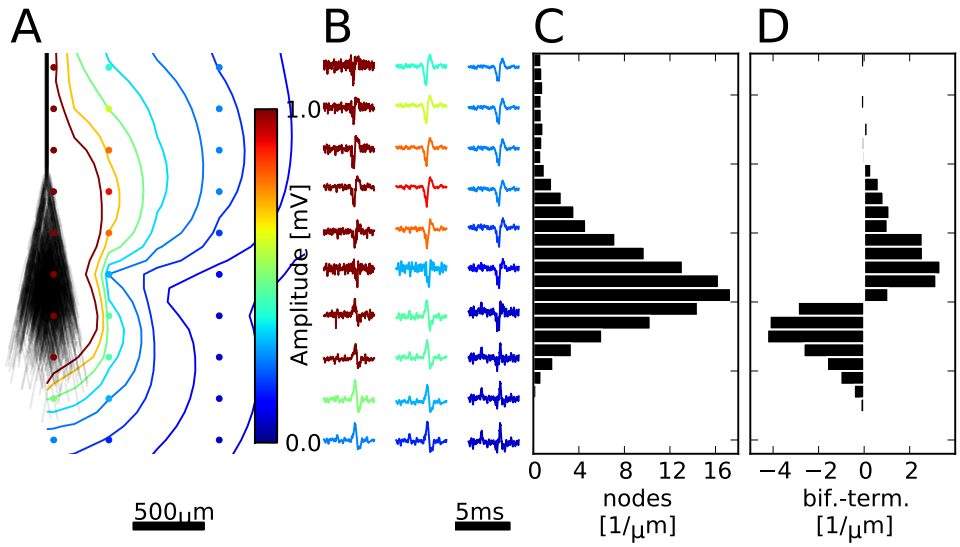

Figure 1: Axonal projections generate a dipole-like extracellular field potential. Extracellular evoked potential due to a pulse of activity in a generic fiber bundle. (**A**) shows the structure of the bundle, next to (**B**) EFP responses at various locations, indicated by colored dots. Scaling of traces indicated by colorbar. Relative strength of high-frequency noise relative to the low-frequency pulse decays with distance. The low frequency pulse switches polarity along the nerve bundles termination zone. (**C**) shows the fiber density overlayed with the strength of the high-frequency EFP component. (**D**) shows the density of bifurcations and terminations at varying depths.

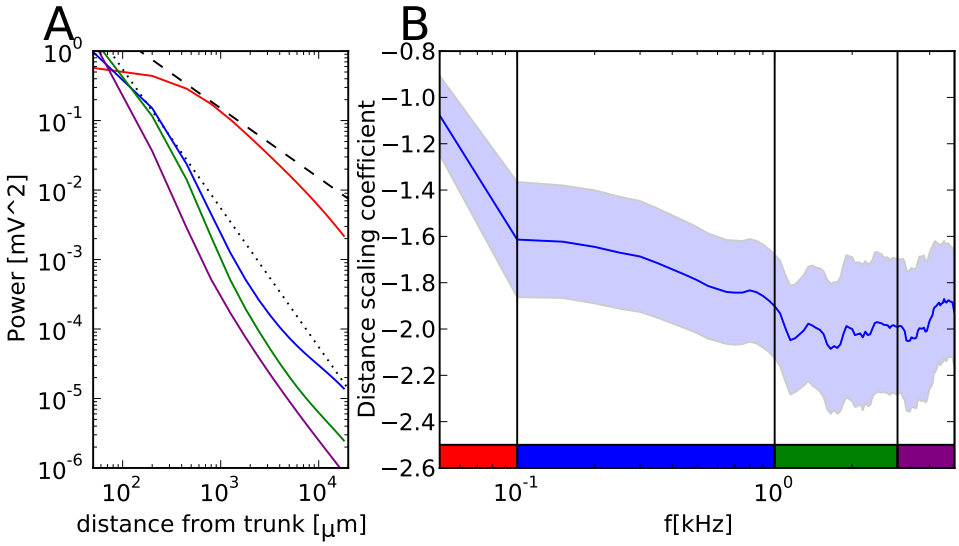

Figure 2: Low-frequency component of the axon bundle EFP exceeds high frequency in reach. (**A**) shows the behaviour of different spectral components (frequency indicated by colorbar) in a double logarithmic plot. The slope indicates the scaling coefficient in this frequency band. (**B**) shows this scaling coefficient for different frequencies. Low frequencies have the least negative coefficient, indicating the furthest reach.

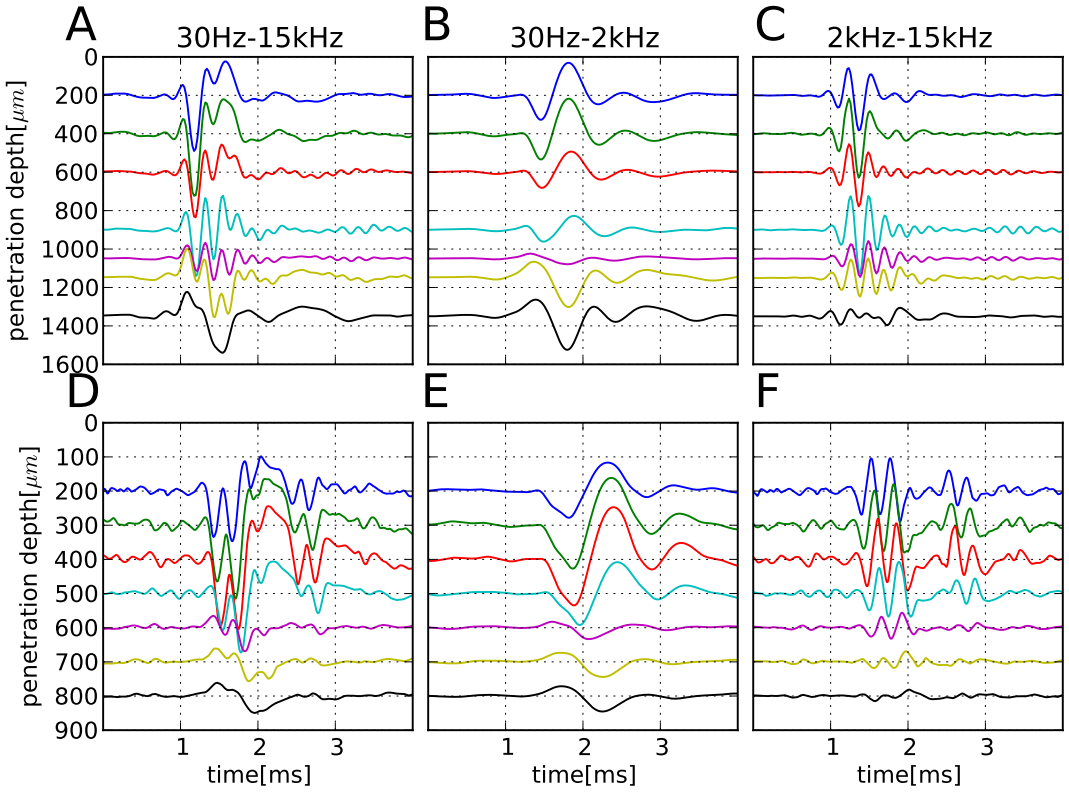

Figure 3: Data from the barn owl shows the expected behaviour predicted by the model. (**A**-**C**) shows data from the barn owls nucleus laminaris in response to an auditory click stimulus, compared to a simulation of the axonal structure and activation in (**D**-**F**). The click stimulus induces a pulse of activity in the afferent axon bundle. The low-frequency components (**B** and **E**) show the polarity reversal. The high frequency component (**C** and **F**), does not show such a reversal, but rather shows a steady increase in phase with depth.

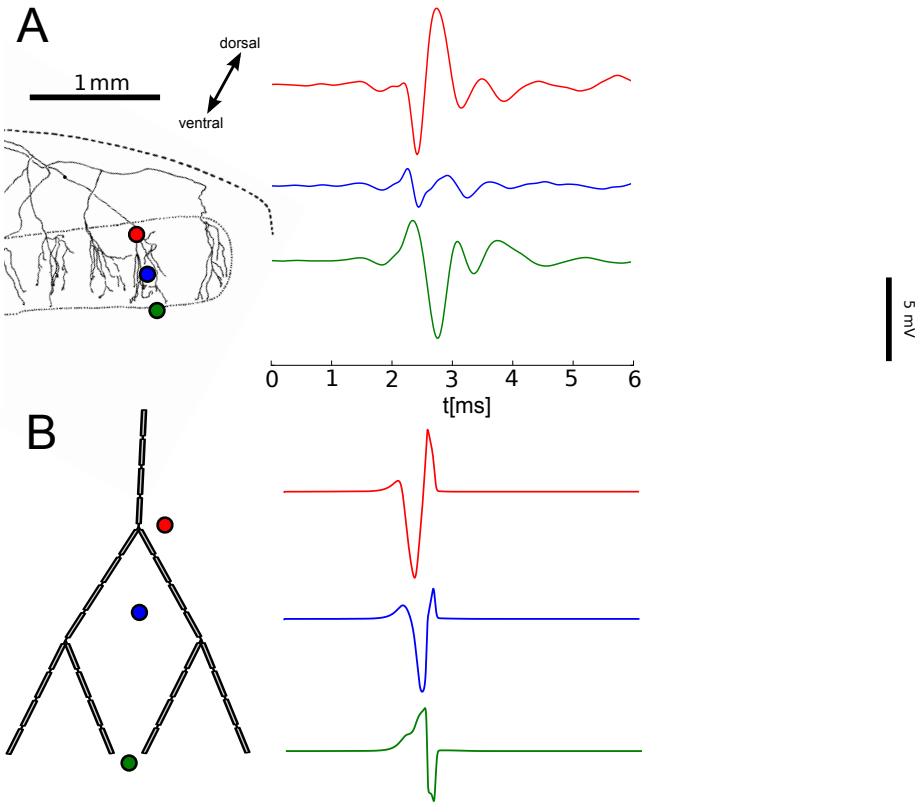

Figure 4: The dipolar behaviour can be understood by examining individual action potentials on a single axon tree. Comparing the low frequency owl data (**A**) to a single axon and action potential in model (**B**) shows a similar behaviour. In particular, the potential at a termination and that at a bifurcation (red and green curves in **B**) are approximately inverted.

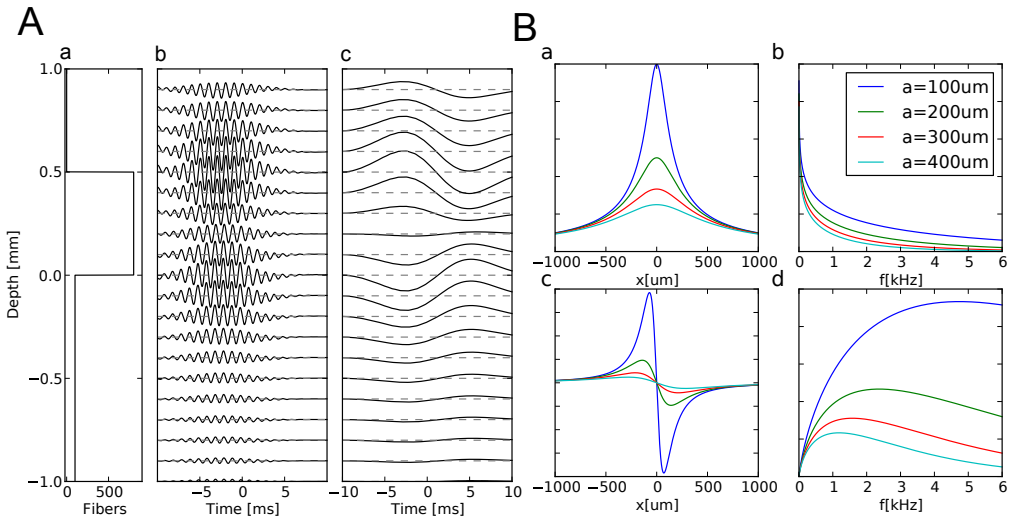

Figure 5: Analytical model of the axon bundle potential explains the effects observed in the numerical model and example data. (**A**) shows the behaviour of a simplified fiber bundle with a piecewise constant fiber density (**Aa**). The high frequency component (**Ab**) shows no polarity reversal, while the high-frequency component (**Ac**) does, as expected from the data and modelling. This can be understood by decomposing the signal into two components. The first component is governed by the bifurcation and termination density, and is filtered by the regular weighting function (**Ba**), which acts as a low-pass filter (**Bb**). The second component is governed by the fiber density, and is filtered by the derivative of the weighting function (**Bc**), which acts as a high- or band-pass filter (**Bd**).

Bibliophraphy

Brette R, Destexhe A eds. (2012) Handbook of Neural Activity Measurement. Cambridge: Cambridge University Press. Available at: http://dx.doi.org/10.1017/cbo9780511979958.

Buzsáki G, Anastassiou CA, Koch C (2012) The origin of extracellular fields and currents — EEG, ECoG, LFP and spikes. Nature Reviews Neuroscience 13:407–420 Available at: http://dx.doi.org/10.1038/nrn3241.

Denker M, Roux S, Lindén H, Diesmann M, Riehle A, Grün S (2011) The Local Field Potential Reflects Surplus Spike Synchrony. Cerebral Cortex 21:2681–2695 Available at: http://dx.doi.org/10.1093/cercor/bhr040.

Einevoll GT, Kayser C, Logothetis NK, Panzeri S (2013) Modelling and analysis of local field potentials for studying the function of cortical circuits. Nature Reviews Neuroscience 14:770–785 Available at: http://dx.doi.org/10.1038/nrn3599.

Gold C, Henze DA, Koch C, Buzsáki G (2006) On the origin of the extracellular action potential waveform: A modeling study. Journal of neurophysiology 95:3113–3128 Available at: http://dx.doi.org/10.1152/jn.00979.2005.

Goodman CS, Bastiani MJ, Doe CQ, Lac S du, Helfand SL, Kuwada JY, Thomas JB (1984) Cell recognition during neuronal development. Science (New York, NY) 225:1271–1279 Available at: http://view.ncbi.nlm.nih.gov/pubmed/6474176.

Gydikov A, Gerilovsky L, Radicheva N, Trayanova N (1986) Influence of the muscle fibre end geometry on the extracellular potentials. 54:1–8 Available at: http://dx.doi.org/10.1007/bf00337110.

Gydikov AA, Trayanova NA (1986) Extracellular potentials of single active muscle fibres: Effects of finite fibre length. 53:363–372 Available at: http://dx.doi.org/10.1007/bf00318202.

Hentschel HGE, Ooyen A van (1999) Models of axon guidance and bundling during development. Proceedings of the Royal Society of London B: Biological Sciences 266:2231–2238 Available at: http://dx.doi.org/10.1098/rspb.1999.0913.

Holt GR, Koch C (1999) Electrical Interactions via the Extracellular Potential Near Cell Bodies. Journal of Computational Neuroscience 6:169–184 Available at: http://dx.doi.org/10.1023/a:1008832702585.

Kandel ER, Schwartz JH, Jessell TM, Others (2000) Principles of neural science. McGraw-Hill New York.

Kuokkanen PT, Wagner H, Ashida G, Carr CE, Kempter R (2010) On the origin of the extracellular field potential in the nucleus laminaris of the barn owl (Tyto alba). Journal of neurophysiology 104:2274–2290 Available at: http://dx.doi.org/10.1152/jn.00395.2010.

Lindén H, Pettersen K, Einevoll G (2010) Intrinsic dendritic filtering gives low-pass power spectra of local field potentials. Journal of computational neuroscience 29:423–444 Available at: http://dx.doi.org/10.1007/s10827-010-0245-4.

Lindén H, Tetzlaff T, Potjans TC, Pettersen KH, Grün S, Diesmann M, Einevoll GT (2011) Modeling the Spatial Reach of the LFP. Neuron 72:859–872 Available at: http://dx.doi.org/10.1016/j.neuron.2011.11.006.

Nornes HO, Das GD (1972) Temporal pattern of neurogenesis in spinal cord: cytoarchitecture

and directed growth of axons. Proceedings of the National Academy of Sciences of the United States of America 69:1962–1966 Available at: http://view.ncbi.nlm.nih.gov/pubmed/4114859.

Nunez PL, Srinivasan R (2006) Electric Fields of the Brain. Oxford University Press. Available at: http://dx.doi.org/10.1093/acprof:oso/9780195050387.001.0001.

Plonsey R (1977) Action potential sources and their volume conductor fields. Proceedings of the IEEE 65:601–611 Available at: http://dx.doi.org/10.1109/proc.1977.10539.

Rattay F, Danner SM (2014) Peak I of the human auditory brainstem response results from the somatic regions of type I spiral ganglion cells: Evidence from computer modeling. Hearing research 315C:67–79 Available at: http://view.ncbi.nlm.nih.gov/pubmed/25019355.

Reimann MW, Anastassiou CA, Perin R, Hill SL, Markram H, Koch C (2013) A Biophysically Detailed Model of Neocortical Local Field Potentials Predicts the Critical Role of Active Membrane Currents. Neuron 79:375–390 Available at: http://dx.doi.org/10.1016/j.neuron.2013.05.023.

Schüz A, Braitenberg V (2002) The Human Cortical White Matter. In: Cortical areas (Schüz A, ed), pp 377–386. Abingdon, UK: Taylor & Francis. Available at: http://dx.doi.org/10.4324/9780203219911/_chapter/_16.